Marker experiments for diffusion in the silicide during oxidation of PdSi, Pd_2Si, $CoSi_2$, and $NiSi_2$ films on ⟨Si⟩

M. Bartur and M-A. Nicolet
California Institute of Technology, Pasadena, California 91125

(Received 22 November 1982; accepted for publication 9 March 1983)

Inert markers (evaporated tungsten and ion implanted Xenon) were used to investigate the mass transport through a silicide layer on a ⟨Si⟩ substrate during thermal oxidation at 700–900 °C. The SiO_2 growth from PdSi, Pd_2Si, $CoSi_2$, and $NiSi_2$ films on ⟨Si⟩ is a process limited by the diffusion of the oxidant from the ambient gas to the silicide/oxide interface. Possible diffusion processes through the silicide that supply Si to the growing SiO_2 layer, but keep the silicide stoichiometry intact, are discussed. Backscattering spectrometry is used to monitor the marker position in the silicide layer. We find that the diffusing species during oxidation correlate with the moving species during silicide formation.

PACS numbers: 81.60.Bn, 68.55. + b, 66.30.Fq, 66.30. − h

I. INTRODUCTION

Thermal oxidation of thin metal silicide films on a Si substrate generally results in the growth of a SiO_2 layer on top of the silicide (Ref. 1, Table XVII). Except for $HfSi_2$, all silicides investigated so far conform to that behavior. In this paper, we consider the silicides of Co($CoSi_2$), Ni($NiSi_2$), and Pd(Pd_2Si and PdSi) which were all reported to have the following characteristics[2,3]:

(a) The SiO_2 layer growth is parabolic with time.

(b) The silicide retains its thin-film configuration and its phase (crystal structure) up to a certain SiO_2 thickness that depends on the initial silicide thickness.

(c) The oxide growth rate is independent of the silicide thickness.

(d) The orientation or the crystalline quality of the Si substrate does not affect the kinetics (in Co and Ni cases). Platinum silicide is an obvious fourth member in this group, but as we have shown[4] it does not follow the same characteristics. An important conclusion from the above observations is that the oxidation process is limited by the diffusion of oxygen-containing species through the SiO_2 layer. As the SiO_2 layer grows, there is necessarily an overall displacement of the Si with respect to the metal. To see that, consider for example, the top interface of the silicide. Before oxidation there is no Si above that interface, but after oxidation Si (in form of SiO_2) resides on top of the silicide. The question addressed here is: How does this displacement of one specie against the other take place? To answer this question we shall first assume that a transport process that is effective for a given species will be so across the whole silicide layer. This assumption is consistent with the fact that the silicide remains stoichiometric during oxidation.

To start we shall assume that only the Si or only the metal diffuse via one process. The possible cases are:

(a) Dissociation of the silicide at the silicide/SiO_2 interface. As the oxygen arrives there it reacts with the Si and frees metal atoms. This excess metal finds its way to the silicon substrate, where it reacts again with Si, thus preserving the silicide. Here we distinguish the two limiting cases:

(i) Metal diffuses through the silicide layer to the silicon substrate by a folding mechanism (i.e., interstitially, through grain boundaries (GB) or any other equivalent process).

(ii) Metal diffuses through the silicide layer toward the silicon substrate by a lattice diffusion mechanism (i.e., substitutionally, or any other equivalent process).

This particular subdivision of diffusion processes is suggested by the experimental techniques. It has been previously used by other authors and is discussed in detail in Appendix A.

(b) No dissociation of the silicide layer. The silicon in the SiO_2 is supplied from the Si substrate to the silicide/oxide interface by either:

(i) A folding mechanism (e.g., direct interstitial or grain boundary diffusion of Si through the silicide layer).

(ii) A lattice diffusion mechanism (e.g., vacancy diffusion of Si through the silicide layer).

We have here four cases: the Si or the metal moves by either a lattice diffusion or folding mechanism. Before discussing more general cases, we consider how these four cases can be distinguished by certain marker experiments.

Backscattering spectrometry (BS) is naturally suited for the measurement of atomic distribution profiles in surface layers a few thousand Å thick. BS can also give the amount of material positioned with respect to one or the other side of a given plane that is delineated by some particular atomic species. It is assumed that these elements do not participate in the process investigated ("inert markers" experiment). This kind of marker experiment combining inert markers and BS thus yields the net mass transported an imaginary plane imbedded in the silicide. In terms of the limiting cases considered above, this experiment thus distinguishes only between the two cases of metal transport versus Si transport, that is, between dissociation or no dissociation [see Fig. 1(a)]. In Fig. 1, we schematically describe the effects of progressive oxidation on our samples, i.e. after a thin oxide growth (short oxidation) and after a (exaggerated) long oxidation process.

The details of the transport mechanisms ("folding" versus "lattice diffusion" mechanisms) are not resolved by an inert marker experiment. To get the full picture, one has to resort to additional analytical techniques. One such tech-

 0021-8979/83/095404-12$02.40

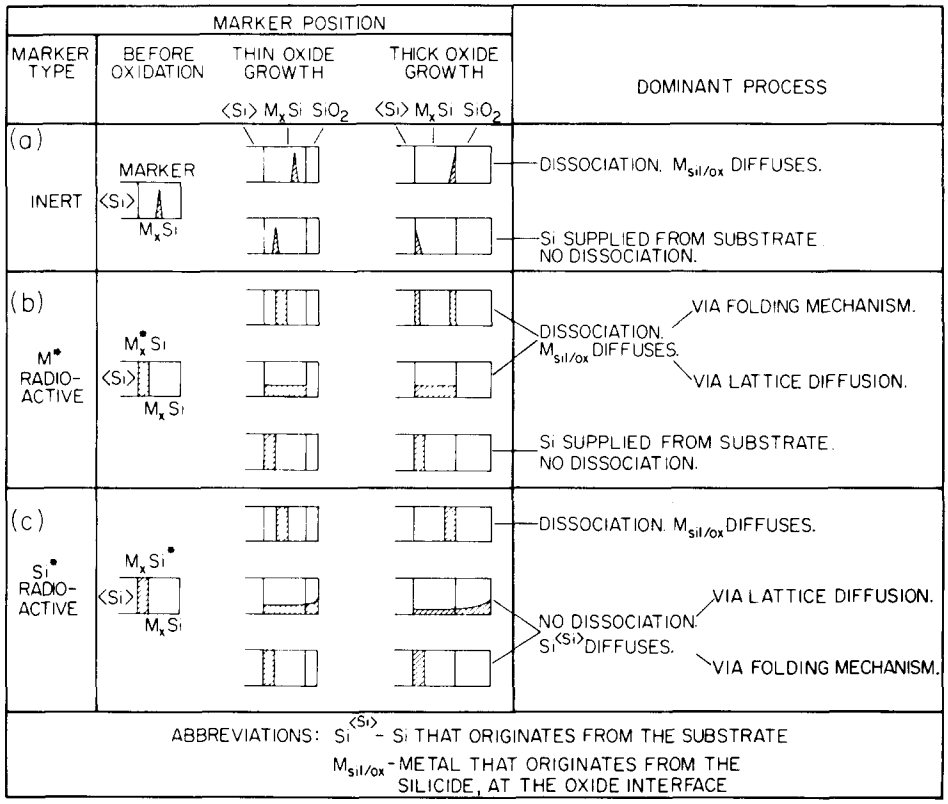

FIG. 1. Comparison between the behavior of three different diffusion markers in the silicide: (a) inert, (b) radioactive metal, (c) radioactive Si, for four cases of mass transport across the silicide induced by the formation of SiO_2, under the assumption that only one specie diffuses via one mechanism. The mechanisms of lattice diffusion and folding are defined in Appendix A.

nique uses a radioactive tracer. In this case, one of the species (metal or Si) has a spacially distinct layer in which a radioactive isotope of that specie is present. The location of this isotope can be monitored. The evolution of that radioactive tracer layer during oxidation reflects the transport process. In Figs. 1(b) and 1(c), we depict idealized radioactivity depth profiles of a tracer layer imbedded initially in the silicide. These profiles are for idealized limiting cases assuming that only one species diffuses and that only one process is responsible for the transport. The above analysis holds also for silicide formation. Appendix A elaborates on the origin of these profiles. The important conclusion is that the diffusion process of the moving species is resolved by the tracer technique. Some treatments of radioactive tracer experiments[5–8] have ignored the intermixing that is inherent in lattice diffusion so that the outcome of lattice diffusion of the marked species was omitted.

To proceed beyond the simple cases described so far, we now consider the general case of a simultaneous diffusion of both Si and metal across the silicide. This may come about as a superposition of the simple cases of (a) metal diffusion toward the substrate, and (b) Si diffusion toward the SiO_2 described above. This particular combination of elemental processes is shown schematically as process B in Fig. 2. In this process, the two species diffuse in opposite directions. There exist three more possibilities: diffusion of the two species in the same direction either inward or outward, and inward diffusion of Si with outward diffusion of metal. This last possibility should be ruled out because it is incompatible with the growth of SiO_2 and the preservation of a stoichiometric silicide layer. The other two possibilities are shown schematically in Fig. 2 as processes A and C.

Figure 2 also indicates the expected shift of an inert marker signal from its initial position E_{Mi} in the energy space of a backscattering spectrum for the three processes A, B, and C. Each of these three cases covers a range of inert marker positions as the relative magnitude of the two atomic fluxes vary. In process A, metal diffuses inwards as a result of the silicide dissociation and some Si also diffuses inward toward the substrate. The source of this Si is the silicide dissociation also, and its transport is the result of a low recombination probability with the diffusing metal. In process C, metal as well as Si diffuse outward toward the oxide. Although this process is unlikely to occur as a result of oxidation, it is included here for the sake of completeness. A further linear combination of the processes A, B, and C is also conceivable, but inert marker experiment will only detect the net resulting effect. The outcome must fall within the realm of one of these processes. It is this net effect that we characterize as a result of inert marker experiment.

In contrast to an inert marker position, the profile of a radioactive tracer cannot in general be interpreted uniquely when more than one process is effective. As shown in Appendix A, the result of tracer experiment will identify a class of processes uniquely only if it is known that a single process is present.

The primary question is whether or not the silicide dissociates at the silicide/SiO_2 interface. This question can be answered by an inert marker experiment while a tracer experiment does not necessarily provide an answer. The optimum procedure for a transport study of this kind is thus to begin with an inert marker experiment and then to proceed with a radioactive tracer of the moving species. In the case where both elements diffuse, two radioactive experiments—

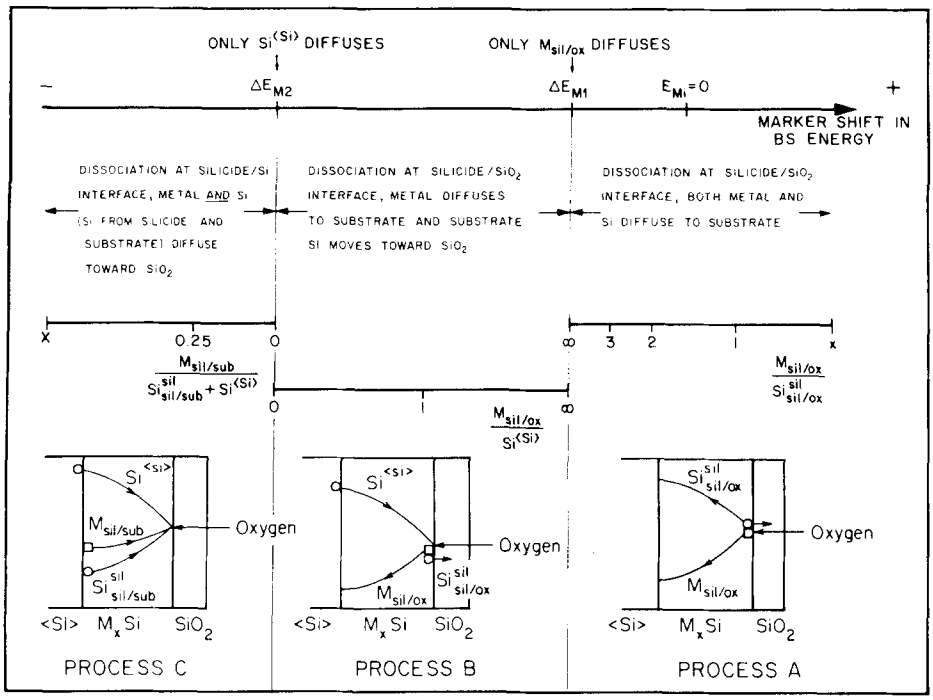

FIG. 2. Schematic scales for the shift of the inert marker BS energy due to the following processes: (A) Both Si and metal diffuse inwards from the silicide/oxide interface toward the substrate. (B) Metal diffuses inwards as in case A, but Si diffuses outwards from the substrate to the oxide. (C) Both Si and metal diffuse outwards from the substrate interface to the oxide interface. The last possible process where the metal moves outwards and Si inwards is omitted because it does not conserve the silicide during oxidation as is experimentally observed.

one with each marker specie—are required.

Accordingly, we report here on first experiments with inert markers to investigate transport in silicide during silicide oxidation. The three possible conclusions are: (i) only metal diffuses (case a), (ii) only Si diffuses (case b), (iii) processes A, B and C (in Fig. 2) where both species diffuse.

A clear distinction between these various possibilities demands high experimental accuracy. Whether or not the silicide dissociates at the silicide/SiO_2 interface is easier to answer and is the first step in understanding the oxidation process. We shall therefore address the dissociation question primarily, and only secondarily, the details of the flux composition.

The following list of abbreviations will be used throughout the paper:

- $Si^{\langle Si\rangle}$ — Si that diffuses from the substrate.
- $Si^{sil}_{sil/ox}$ — Si that diffuses from the silicide at the silicide/oxide interface.
- $Si^{sil}_{sil/sub}$ — Si that diffuses from the silicide at the silicide/substrate interface.
- $M_{sil/ox}$ — Metal that diffuses from the silicide at the silicide/oxide interface.
- $M_{sil/sub}$ — Metal that diffuses from the silicide at the silicide/substrate interface.
- ΔE_M — Net change of marker position in BS spectra. ($\Delta E_M = E_M - E_{Mi}$; E_M—marker's BS energy after oxidation; E_{Mi}—initial marker's BS energy).

II. EXPERIMENTAL AND ANALYTICAL PROCEDURES

An inert marker for the investigation of the oxidation process of a silicide layer should be imbedded inside the silicide in the form of a well-defined layer, desirably at the center of the film. It is known that for Co and Ni, metal is the dominant diffusing species in the first silicide phases formed (Ref. 1, Table VIII). To have the marker finally situated inside the silicide layer, it must therefore be imbedded first in the silicon. We incorporated the two different markers, Xe and W, differently.

The tungsten marker was prepared by sequential e-gun evaporation on top of the Si single-crystal substrate of W (5–15 Å-thick), Si, and finally the metal, followed by appropriate thermal annealing. The amorphous silicon thickness was adjusted so that after silicide formation the marker was imbedded in the silicide. All Si substrates were *n* type with ⟨111⟩ orientation. The deposition was conducted in an ion-pumped e-gun evaporator at a pressure below 2×10^{-7} torr. The annealing was done in a vacuum furnace at a pressure below 10^{-6} torr, at 800 °C for Ni and Co (to form $NiSi_2$, $CoSi_2$), or 750 °C and 850 °C for Pd (to form Pd_2Si and PdSi, respectively). At this temperature W should form WSi_2 which is the actual inert marker. We did not confirm that phase due to the sensitivity limitations of the analytical techniques available to us.

The Xe marker was implanted in the Si substrate. We chose Xe because its heavy mass assures good sensitivity and signal separation in a BS spectrum and due to the anticipated formation of bubbles. The doses were $2\text{–}5\times10^{15}$ cm^{-2}. Previous studies of Ne, Ar, and Kr implanted in Si[9,10] show that at such doses ideal gases form microbubbles in the Si and will not diffuse out during the following heat treatment. The observed trend is that the higher the mass is, the lower the required dose for bubble formation becomes. We thus expect to form Xe bubbles at this 600 keV Xe implantation. To check the stability of Xe in Si, we oxidized the implanted Si wafers at 900 °C for 20 min. There was no spread of the Xe signal and the total amount was conserved. Other samples were only cleaned in a plasma of O_2. The thin oxide was then

etched away with HF. The metal was e-gun evaporated, followed by vacuum annealing, both under the same conditions as for the W marker.

The oxidation was conducted in an open tube furnace in dry O_2 or wet (O_2 bubbled through 95 °C H_2O). These are the same conditions under which we previously characterized the kinetics of silicide oxidation.[2,3,11]

As a check for the inert quality of our marker we compared the oxidation kinetics of samples with and without marker. This check was conducted in each case. Thermal annealing in vacuum instead of an oxidizing ambient, for the same time/temperature cycles as in the oxidization case, was also conducted. This experiment tests the stability of the marker when mass transport is absent in the silicide. If there were a driving force to change the marker position that is unrelated to the mass transport generated by the oxidation process, it would show up as a marker shift after this vacuum annealing. The kinetics studies and inert ambient annealings confirmed the passive nature of our markers.

As an analytical tool we used BS spectra of 2 MeV $^4He^+$ at normal incidence and the detector at a 170° scattering angle. This technique measures the total energy that a helium ion loses as it penetrates to the marker, undergoes an elastic collision, and then loses energy again on its way out to the detector. The changes of this energy loss reflect the amount of material removed or added in front of the marker. Since we know that only oxygen is incorporated in the growing SiO_2 layer, and that the silicide remains stoichiometric, the position of the marker signal in the energy space of a BS spectrum can be converted uniquely to a position of the marker in the real space of the silicide. To clarify the result of this conversion, we describe in Fig. 2 the energy shifts of a marker signal in a BS spectrum as a result of various transport processes. In this figure we have set the energy E_M of the marker signal at its initial value E_{Mi} before oxidation as 0. The upper line gives the shift of the marker signal in the energy space of BS spectrum. Below it we designate regions of markers energy shift that correlate with transport processes described before, for a given oxide thickness. For each of the processes considered, a ratio scale is given that indicates the ratio of atomic fluxes involved.

ΔE_{M1} is the marker position when the silicide dissociates at the silicide–oxide interface, when all the Si is oxidized and when only metal diffuses. In this special case, silicide dissociates at the SiO_2 interface and generates excess metal that can move to the substrate, hence reducing the stopping power in front of the marker. But the oxygen incorporated in the SiO_2 increases the stopping power. The net effect of both yields a shift of energy ΔE_{M1}.

ΔE_{M2} is the position of the marker when only Si diffuses from the substrate through the silicide to the oxide interface where it is oxidized. In this case, Si adds stopping material in front of the marker. This contribution adds to that of the incorporated oxygen and causes the shift of ΔE_{M2}.

The position of a marker in general is calculated in Appendix B. Numerical values for the silicides considered in this paper per 1000 Å SiO_2 and a heavy marker are also depicted in Appendix B.

III. RESULTS

Table I describes the set of experiments conducted and gives the main results. Details are discussed below in the order of the listing in that table.

A. PdSi

The as-evaporated sample consisted of the following layers (on a ⟨111⟩ Si substrate): 15 Å W, 680 Å Si, 1200 Å Pd. After vacuum annealing at 400 °C for 30 min about 2000 Å Pd_2Si was formed. The W signal was spread, but centered at the Pd_2Si/Si interface. This is expected if during Pd_2Si formation Si is the dominant diffusing specie.[12] Our sample preparation procedure confirmed that. Final annealing for 30 min at 800 °C in vacuum transformed the Pd_2Si to PdSi. The marker position in the as-prepared sample is described in Fig. 3. The marker is situated well within the silicide. From this marker position, we conclude that there was no interface drag of the marker in the Si/silicide interface, and that during PdSi formation Pd is a moving specie. To verify the marker stability, we checked the marker position after an additional 12 min at 850 °C in vacuum. No marker

TABLE I. Summary of the experimental results.

	Characteristics of silicide studied		Inert marker experiment		
Silicide	Existence[a] temperature range °C	Oxidation[b] temperature range °C	Marker Type	Temperature of oxidation °C	Result
PdSi	~800–853 °C	820–850 °C	W	850 °C Wet	Dissociation
Pd_2Si	up to ~800 °C	~750 °C	W	750 °C Wet	No dissociation (?)
$CoSi_2$	up to ~1150 °C	700–1100 °C	W	800 °C Wet	Dissociation
			Xe	850 °C Wet	Dissociation
$NiSi_2$	up to ~963 °C	700–940 °C	Xe	850 °C Wet 900 °C Dry	Dissociation
			Thick W	900 °C Dry	Dissociation

[a] The existence temperature range was extracted from Ref. 1.
[b] and the oxidation temperature range from Refs. 2, 3, and 11.

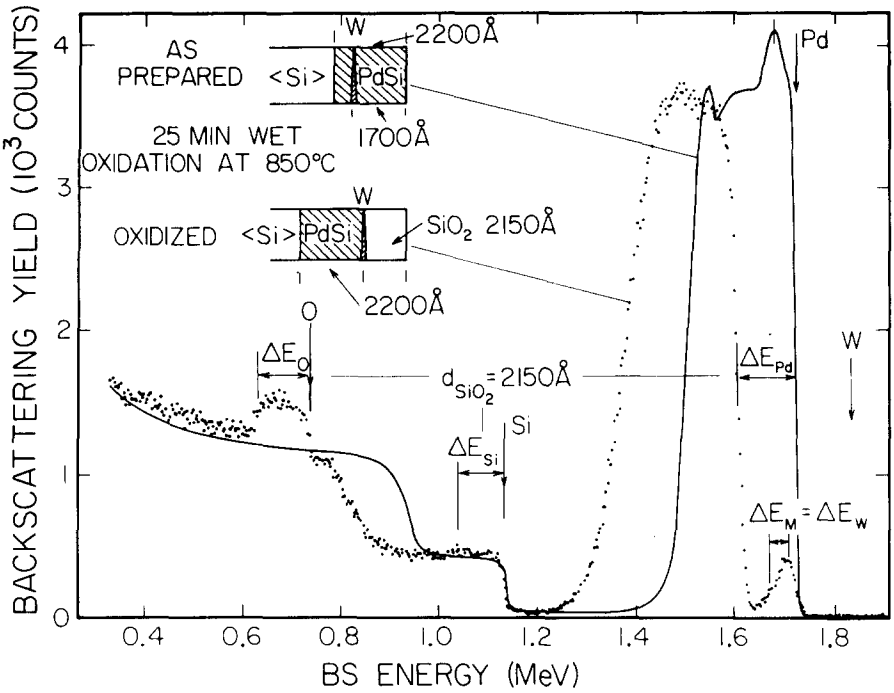

FIG. 3. 2 MeV $^4He^+$ BS spectrum of a PdSi layer with a W marker imbedded in the silicide (probably in WSi_2 form), before oxidation (solid line) and after 25 min, 850 °C wet oxidation (dots). Pd, Si, and O energy shifts give the SiO_2 thickness. The relative marker shift ΔE_M is 10 keV/kÅ.

shift was observed. Figure 3 gives the BS spectrum of the as-prepared PdSi sample compared to a spectrum taken after 25 min of wet O_2 oxidation. This figure also serves as an example of the way we analyzed the BS spectra. From the shift of the metal signal (in this case, ΔE_{Pd}) and the widths ΔE of the Si and O signals, we find the SiO_2 thickness with an accuracy of about $\pm$ 50 Å. The shift ΔE_M of the marker in keV (22 keV in our case) is then divided by the oxide thickness (2150 Å) to give the relative marker energy shift of 10 keV/kÅ. From Appendix B, we find that this value corresponds exactly to ΔE_{M1} which is dissociation process with metal diffusion to the Si substrate. We conclude that silicide dissociates at the SiO_2/silicide interface. However, caution should be exercised since in this example we have an extreme case where finally the marker resides at the silicide/oxide interface. An alternative scenario is that the marker actually shifted rapidly until it reached the SiO_2/silicide interface. This motion corresponds to process A in Fig. 2, which again implies dissociation so that the conclusion is the same.

B. Pd_2Si

Sample preparation for this experiment is exactly as described for the PdSi case, but without the final annealing step of 30 min at 800 °C. The W marker was centered at the Si/silicide interface. The oxidation was done at 750 °C with wet oxygen atmosphere. This low temperature was chosen to ensure that during oxidation there will be no phase transition in the silicide. As reported,[3] oxidation of Pd_2Si at 750 °C results in formation of SiO_2 on top, but also some Pd_xO is formed on the surface, depending on the history of the sample. Due to this complicating fact, we do not present BS spectra, but summarize the results in Fig. 4. The marker position is obviously shifting down in energy. We get about $-$ 56 keV/kÅ. Using the scale of Appendix B, we find that the marker shift matches ΔE_{M2}. Stated differently, the result is that the W marker stays at the Si/Pd_2Si interface. This can be the effect of an interface drag that controls the marker position and not the true atomic transport. We can refer to the PdSi experiment where the marker was shifted from that interface so we do not expect the drag to control the marker position. Hence, we tentatively conclude that Si is the moving specie during the silicide oxidation and there is no dissociation.

C. $CoSi_2$

1. Thin Tungsten Marker

The sample as evaporated consisted of the following layers (on a ⟨111⟩ Si substrate): ~6 Å W, 1100 Å Si, and 550 Å Co. Vacuum annealing cycles of 30 min at 400 °C and 30 min at 800 °C concluded the sample preparation. The marker thus formed was imbedded 1300 Å-deep in the silicide. (See schematic description in Fig. 5). We performed a series of oxidations for 5, 20, 45, 80 and 125 min at 800 °C in wet O_2. The resultant oxide thicknesses were 490, 1080, 1570,

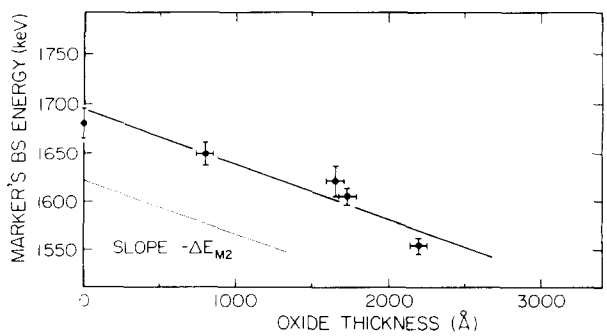

FIG. 4. Tungsten marker energy in BS spectrum of Pd_2Si sample as a function of the oxide grown on top. Oxidation was done at 750 °C wet. The heavy line slope is $-$ 56 keV/kÅ, which corresponds (see Appendix B) to dissociation with metal diffusion toward the substrate, if there is no interfacial drag.

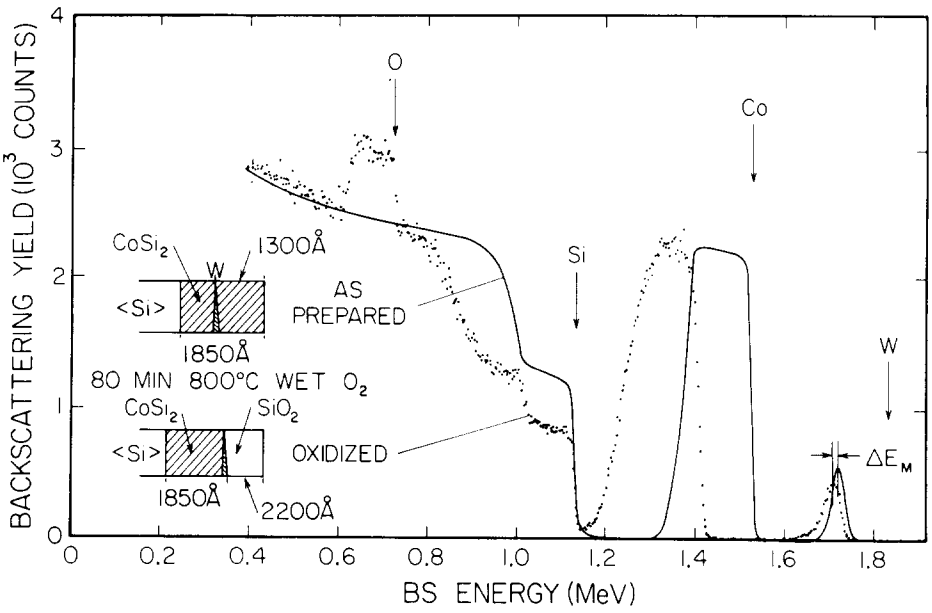

FIG. 5. 2 MeV $^4He^+$ BS spectrum of a $CoSi_2$ layer with a W marker imbedded in the silicide, before oxidation (solid line) and after 80 min, 800 °C wet oxidation. The relative marker shift ΔE_M is -5 keV/kÅ.

2200 and 2770 Å, respectively. The parabolic rate constant thus obtained fits exactly the $CoSi_2$ oxidation kinetics reported previously in Ref. 2, Fig. 1. The marker position in BS energy space almost did not change during the oxidation. For example, we depict in Fig. 5, the BS spectrum after 80 min oxidation, which is exactly when the marker reaches the SiO_2 interface. Only about -10 keV marker shift is observed. The argument previously raised in the PdSi case does not apply here because we have checked the marker position intermittently and saw no significant shift all the way. Using the scale in Appendix B, we find that the marker shift corresponds to process A which is dissociation at the silicide/SiO_2 interface followed by diffusion of both metal and Si toward the substrate. The essential result of this experiment is that it indicates dissociation. The energy resolution for the marker position is not high enough to quote a fixed ratio of $Co_{sil/ox}$ to $Si_{sil/ox}$ in the fluxes toward the ⟨Si⟩ substrate. $\Delta E_M = -5$ keV/kÅ corresponds to about $Co_{sil/ox}/Si_{sil/ox} \simeq 2$. The average marker shift of all samples in the sequence combined is about -8 keV/kÅ. To check our result, we repeated the experiment with samples that had 3400 Å thick $CoSi_2$ layer where the marker was imbedded 2750 Å deep inside the silicide. We got exactly the same oxide thickness with the marker moving slightly more down, about -15 keV/kÅ.

The result we extracted from these data is a definite dissociation of the silicide at the SiO_2 interface with Co indiffusion and possibly some Si movement in the same direction.

2. Implanted Xenon Marker

The substrate of this sample was implanted with 3.8×10^{15} Xe atoms/cm^2 of 600 keV, as explained before. About 450 Å Co was evaporated and then vacuum-annealed for 30 min at 400 °C and 30 min at 800 °C. The sample thus formed had a silicide thickness of about 1700 Å, and the Xe marker was imbedded partially in the silicide and partially in the Si substrate. Further annealing at 850 °C in an Ar environment did not change the Xe distribution. Figure 6(a) is the BS spectrum of our sample before oxidation. The Xe signal was magnified, and is rendered in Fig. 6(b). We show the data points and the curve we have fitted to this data. The following figures contain only the fitted curve. (The statistical uncertainty is typically the same for all cases.) In Fig. 6(c), the BS signal of Xe after 850 °C wet oxidation is given for various oxide thicknesses. (Again, the kinetics fit exactly to that of Ref. 2). On each curve we have marked the position of the $CoSi_2/SiO_2$ interface. After 1700 Å oxide was grown, the Xe signal is fully imbedded in the silicide. It is difficult to assign a marker position accurately to this distribution, but we arbitrarily have chosen the maximum height. This gives a marker shift of -15 keV/kÅ. After 2750 Å oxide growth, the Xe is distributed almost equally in the silicide and the oxide. We chose the lower peak which gives a lower limit of Xe position in the silicide. This solution would yield about -12 keV/kÅ marker shift. We included a third curve after 4200 Å SiO_2 was grown on the $CoSi_2$. There is almost no marker shift, but nearly all the marker is imbedded in the SiO_2.

The Xe marker has much less resolving power than the W marker. We nevertheless have two conclusions: First, using the scale in Appendix B, it is clear that silicide dissociation and metal diffusion occurs. We cannot state if any excess Si generated during the dissociation is diffusing back to the substrate. The second observation is that during SiO_2 growth oxygen is the moving species through the SiO_2 layer. This is a well established result[13] and this agreement with our result serves as a further confirmation and validation to this marker experiment. The marker moves through two interfaces (Si/$CoSi_2$ and $CoSi_2/SiO_2$) with practically no change so we conclude that there is no interface interaction or driving force that shift our Xe spectra.

D. $NiSi_2$

1. Implanted Xenon Marker

Our first set of samples for this experiment were done together with the $CoSi_2$ sample we already discussed, on the same substrate, with about 500 Å of evaporated Ni. The

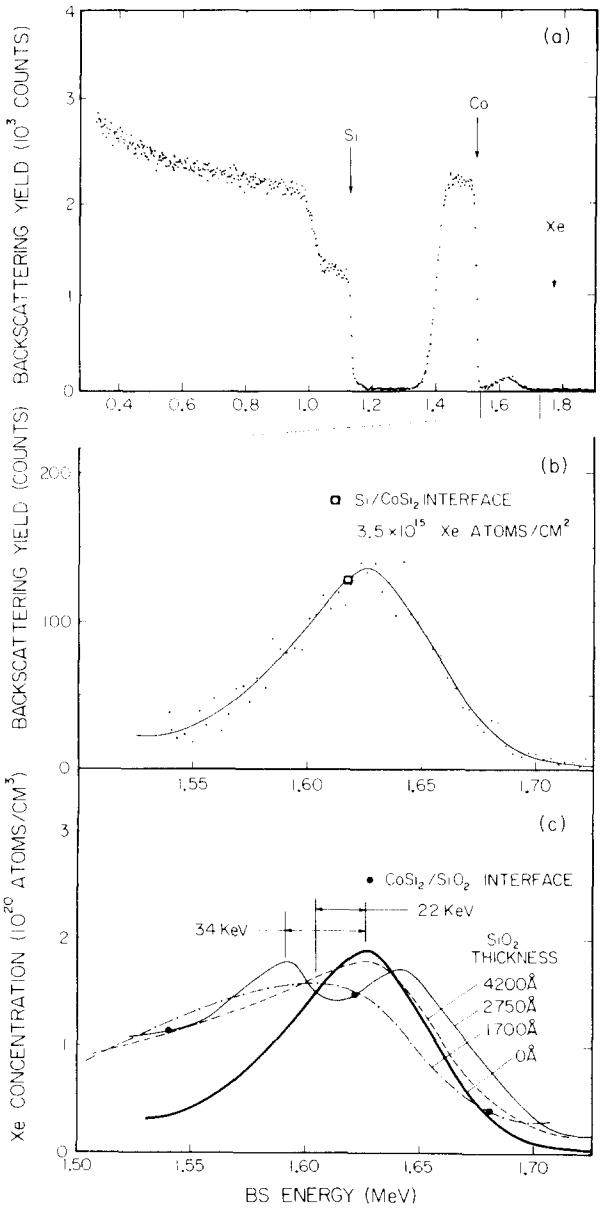

FIG. 6. 2 MeV $^4He^+$ BS spectrum of: (a) $CoSi_2$ layer with Xe marker. (b) The magnified Xe signal and the fitted curve. (c) Overlapped fitted curves of the Xe marker after oxidation. The relative marker shift is more than -14 keV/kÅ.

results after wet oxidation (as was already reported,[11] the kinetics for $CoSi_2$ and $NiSi_2$ oxidation are practically the same) were similar to the $CoSi_2$ and led to the same conclusions. To confirm these results, we repeated the experiment on a freshly implanted sample (5×10^{15} Xe atoms/cm^2) and the oxidation was conducted at 900 °C in dry O_2. The initial silicide layer was about 2000 Å-thick. The Xe marker was predominantly in the Si substrate as described in Fig. 7. Initially, the marker shift does not correspond to our model assumptions. But after some oxidation, the marker resides inside the silicide and can be used for our model.

Figure 7 describes the Xe profiles after successive oxidation. Again, the oxidation rate was the same as reported for samples without marker. The interface between $NiSi_2$/SiO_2 is marked on each of these curves. Except for the initial shift, due to the fact that the Xe was not fully in the silicide initially, all the sample profiles are practically the same. Using the scale of Appendix B, we conclude that dissociation occurs when metal diffuses into the substrate, and that possibly some Si diffuses from the sil/ox interface to the Si substrate.

2. "Thick" Tungsten Marker

The sample preparation here was the same as for the $CoSi_2$-W marker experiment, except that the initial W layer thickness was about 15 Å rather than ~6 Å. Following the W evaporation, we deposited about 1800 Å Si and 750 Å Ni sequentially. The relatively thick W acts as a local barrier between the Si substrate and the growing silicide. Evidently, the W layer is nonuniform, so that the silicide grows in columns located at weak spots of the W layer. A similar method of applying W island structure as a diffusion marker has previously been reported.[14] In Fig. 8, we schematically describe our sample preparation and its resulting morphology. Again, we expect the W to be bonded to Si in the WSi_2 form. The BS spectrum of the as-prepared sample is depicted in the figure as a solid line. The area blocked by the W layer is almost 30% of the interface.

This sample construction enables us to get more information from the BS spectra than is usually achieved with a marker experiment. Since the marker leaves a clear trace in the Ni signal, we can also find the amount of Ni above the marker. From signal heights we confirm that the compound above the marker is $NiSi_2$. The amount of Ni above the W becomes an additional independently measured quantity. Since the silicide stays stoichiometric and the SiO_2 thickness can be obtained independently, we can separately determine the total amount of Ni and Si that resides above the marker. The dotted spectrum in Fig. 8 serves as an example. From the shift of the Ni signal and the difference of the Si and O width (in the SiO_2 signal), we obtained the SiO_2 thickness that is, the amount of Si in the oxide. From the W marker step in the Ni signal, we find the total amount of the Ni above the marker. Since we know that the compound is $NiSi_2$, the total Si amount above the marker is twice that of the Ni plus the silicon contained in the oxide. In Fig. 9, we show the result of this analysis as deduced from the spectra. All samples were oxidized at 900 °C, those marked *S* were done in wet O_2 and the rest in dry O_2. (Again, the kinetics fit the "nonmarker" case.) It is clear that both Ni and Si are lost above the marker, so that process A of Fig. 2 applies. Here we can be quantitative and check the slopes to get the flux ratio $M_{sil/ox}/Si_{sil/ox}$ of the two diffusing species. The ratio can be determined independently from the Si and Ni slopes and is consistently found to be about 2, which is in good agreement with the Xe marker results.

IV. DISCUSSION

The results as summarized in Table I clearly indicate dissociation in the PdSi, $CoSi_2$, and $NiSi_2$. The general trend we find is that some Si also diffuses from the sil/ox interface

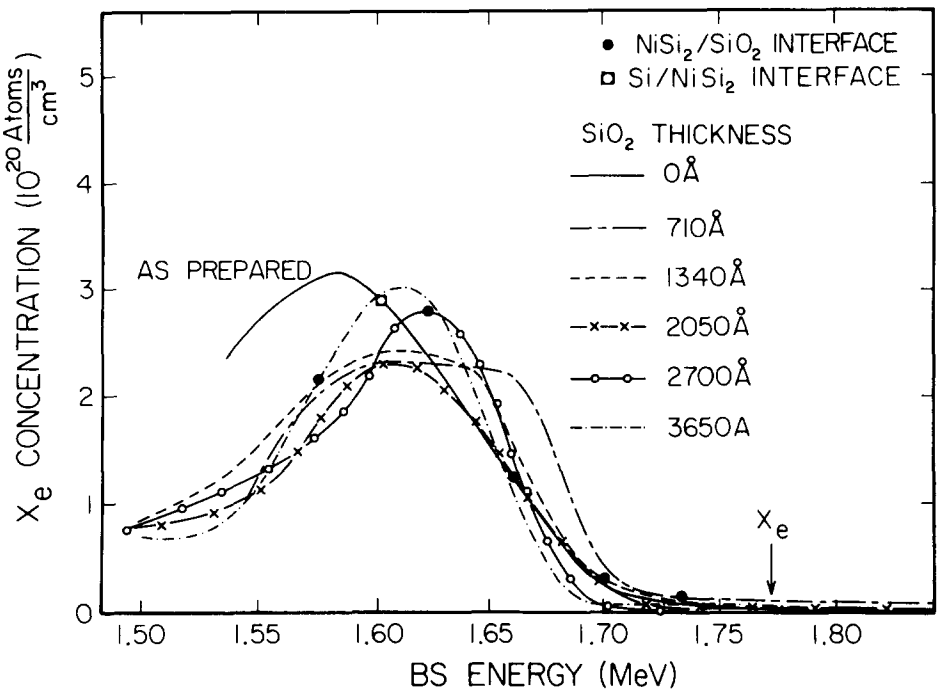

FIG. 7. 2 MeV $^4He^+$ BS spectrum of a Xe marker imbedded in a $NiSi_2$ layer. The sequence describes the Xe profile for different oxide thicknesses after 900 °C dry oxidation. Although complex in details, the plots demonstrate that within the accuracy of the measurements, there is no shift of the implanted Xe marker during oxidation. (The "as-prepared" profile is shifted a little bit down in energy due to its position under the initial sil/SiO_2.)

down to the substrate. The simple explanation we suggest is as follows: The oxidation process is controlled by the oxygen arrival at the sil/ox interface. All other processes apparently are much faster and do not influence the kinetics. Oxygen arrival at the interface breaks up the silicide bonds and generates an excess of metal and Si. This is a local phenomenon and the probability of silicide reconstruction with the excess Si and metal is low. Hence, both species diffuse toward the substrate. In previous studies,[8] it was found that during $NiSi_2$ formation Ni diffuses substitutionally in the silicide. The substitutional nature of the Ni may contribute to the low reconstruction probability inside the silicide lattice.

As already stated in the introduction, inert markers should be the first, but not the only experimental technique used to resolve the mass transport problem. The next step is to apply the appropriate radioactive tracer to characterize the diffusion mechanism. From our results, it is clear that for this silicide oxidation, where the metal moves predominant-

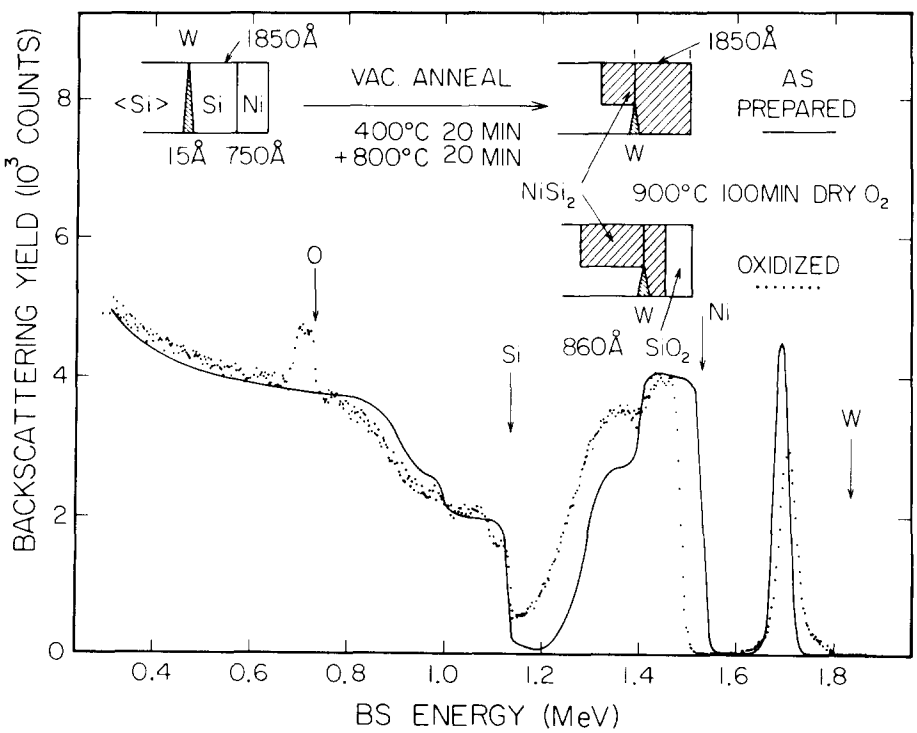

FIG. 8. "Thick" W marker. The 2 MeV $^4He^+$ BS spectrum is analyzed according to the simple model described schematically. Following oxidation, in addition to the information from the marker shift, the total Ni amount above the marker can be obtained. The initial "blocked" surface area is about 30% and after 100 min oxidation is only about 10%.

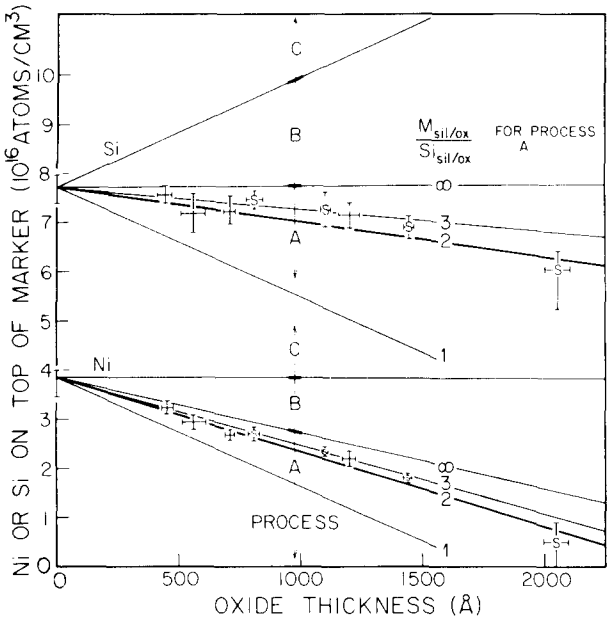

FIG. 9. Nickel and Si concentrations, above the "thick" W marker, as function of the grown SiO_2 thickness. All samples were oxidized at 900 °C; data points marked *S* are for wet, the others for dry O_2 oxidation. The ranges over which the different processes A, B, and C of Fig. 2 apply are indicated. The experimental results show that the $NiSi_2$ dissociates and that both the metal and the silicon (ratio $M_{sil/ox}$ $Si_{sil/ox} \simeq 2$) diffuse inwards to the substrate.

ly, one needs radioactive metal marker experiments. Such an experiment is not reported in the literature. But the oxidation of $CoSi_2$ was studied with a Si tracer experiment.[13] The conclusion was that "silicon diffuses through the silicide by a substitutional (vacancy) mechanism". In the terminology used in our introduction, this conclusion states that $Si^{(Si)}$ mixes with the $Si^{(sil)}$ via lattice diffusion. But the present results show the dominant process is Co transport to the ⟨Si⟩ substrate. The silicon lattice diffusion hence must be a secondary process. The conclusion as stated[13] implies no dissociation and is incorrect.

In the Pd_2Si case, we find that Si is supplied from the substrate and here a radioactive Si tracer experiment would be meaningful and conclusive to identify the mode of Si transport. We cannot exclude dissociation at the oxide interface, however. For example, it could be that the diffusion rate of Si from the substrate in the silicide is much higher than that of the metal while dissociation does occur, so that most of the silicide reconstruction occurs near the oxide interface. (This is basically a variation of process B in Fig. 2 where the metal only moves a short distance into the silicide.)

The question arises what the connection is between the transport across the silicide observed here during oxidation and the transport during silicide formation by reaction of a metal film on Si. We compare the known results from both oxidation and silicide formation in Table II. The table suggests a rule: during oxidation the dominant moving species is the same as in the silicide formation. This result is physically plausible. In silicide formation or oxidation, we deal with the same bulk, hence same relative magnitude of diffusivities.

TABLE II. Dominant diffusion species during silicide formation and oxidation.

Silicide	Dominant diffusion specie during silicide formation	Dominant diffusion specie during oxidation
PdSi	Si and Pd[a]	Pd
Pd_2Si	$Si^{(b)}$; Si and Pd[c]	(Si)
$CoSi_2$	unknown	Co
$NiSi_2$	$Ni^{(d)}$	Ni
$TiSi_2$	$Si^{(e)}$	$Si^{(e)}$

[a] We conclude that, from the position of the marker in our sample described in Fig. 4.
[b] Ref. 12.
[c] Ref. 1.
[d] Ref. 15.
[e] Ref. 16.

Apparently, the boundary conditions generated by the chemical reaction at the interfaces are also similar, which results in similar atomic fluxes in both cases. Oxidation studies are more controllable at high temperature than the formation of silicides. Hence we may infer the moving species in the formation of a silicide from oxidation studies. We thus predict, for example, that Co is the moving species in $CoSi_2$ formation.

ACKNOWLEDGMENTS

The authors wish to thank the reviewer for very constructive criticism of the manuscript, Dr. K. N. Tu of IBM, Yorktown Heights, for his comments, and R. Gorris and R. Fernandez (Caltech) for technical assistance. The work was executed under the UR Fund of the Böhmische Physical Society (B. M. Ullrich), and was partially supported by Solid-State Devices, Inc. (A. Applebaum, President).

APPENDIX A

We discuss diffusion processes through an assumed uniform layer. Such is the case in silicide formation and in our case of silicide oxidation. We are interested in the atomic traffic from one boundary plane of the silicide to the other.

In this Appendix we follow ideas previously proposed for analysis of radioactive tracer studies. All the schematic presentations used by the different authors working in this field to interpret the results of radioactive tracer experiments ignore the thermal random motion of a diffusion process [for example, Refs. (6–8, 13, 16)]. As different authors have used different terminologies, we first define a terminology that generalized the previously used notations.

We subdivide atomic diffusion processes in crystals into two groups. All diffusion processes which involved exchange with lattice atoms are lumped together in a process we call "*Lattice Diffusion*". For the silicides considered here, this type of mechanism amounts to exchanging an incoming diffusing species at one boundary with an outgoing atom of the same species at the other boundary. The second group contains all diffusion processes which change the atomic sequence in the sample (e.g., GB diffusion), which we call

TABLE III. Classification of basic diffusion processes.

	Diffusion Process[a]	Basic mechanism
Defect independent	1) Direct Exchange	Lattice diffusion
	2) Ring Mechanism	Lattice diffusion
Interstitial	1) Direct Interstitial	Folding
	2) Interstitial	Lattice diffusion
	3) Crowdion	Lattice diffusion
	4) Dissociation	Lattice diffusion
Vacancy	1) Vacancy Distribution	Lattice diffusion
	2) Relaxation	Lattice diffusion
Dislocation		
	1) Pipe Diffusion	Folding
	2) GB Diffusion	Folding

[a] For more details of a specific diffusion process, see for example, Ref. 17.

"*Folding Mechanism*". In a silicide oxidation, this kind of process will generate an inverted sequence in the atomic layers of the diffusing species. The best example is the radioactive marked metal that diffuses through GB. See the top schematic in Fig. 1(b).

To clarify the definition, we have categorized in Table III all diffusion processes in crystals,[17] according to the concepts of lattice diffusion and folding mechanisms.

To include the effect of thermal random motion we must identify which atoms in the layer through which we investigate the traffic are candidates for participation in the random walk process. To have a net transport through a layer, when the total amount of atoms transported is of the same order of magnitude as the total number of atoms in the layer, the diffusion coefficient of the moving species D multiplied by the process duration t must be at least of the same order of magnitude as the square of the layer thickness L ($Dt \sim L^2$). In such a case, no matter what the process is, all the atoms involved in the traffic mechanism are mixed with the incoming flux so that the out-flux consists of atoms from both sources.

For the case of folding mechanism, it is conceivable that the simplified description ignoring thermal random motion holds, because the total number of atoms that participate in the traffic through the layer is small compared to the total number of atoms in the layer. For example, in grain boundary diffusion we consider only atoms that decorate the grain boundaries, and in direct interstitials only the interstitial concentration. In both cases, the exchange with atoms at lattice sites can be ignored (otherwise an additional diffusion mechanism should be invoked). Since most of the radioactive tracer atoms are assumed to be initially located on lattice sites and do not participate in the transport process, the position of the tracer can indeed convey information on the rearrangement of the atoms in the sample. Even when an additional diffusion process—not the dominant one—is included, the geometrical boundary of the radioactive profile can still be identified and serve for analysis. We can thus refine the concept of a folding mechanism as a process in which a substantial fraction of atoms in the layer is excluded from the atomic traffic.

For the case of lattice diffusion, all the atoms in the layer are candidates for exchange so the mixing of the radioactive element in the layer is anticipated. When lattice diffusion is dominant and the transported number of atoms is commensurate with the atoms in the layer, the mixing will be very thorough, so that the radioactivity profile in the layer will be uniform throughout the layer. For example, in Fig. 1(b), we schematically describe the effect of lattice diffusion. The oxide formation at the silicide/oxide interface samples the instantaneous radioactive level in the layer. Since fresh Si is consumed from the substrate and is mixed in the layer, the level within the layer declines. The oxide profile contains the information about the radioactivity level in the silicide layer at each oxide thickness.

In some cases, the presence of a lattice diffusion mechanism can be identified experimentally by profiling in SiO_2 layer, but this tracer profile does not assure that the Si lattice diffusion is the dominant diffusion process. It might only be a secondary process. (See our discussion on the $CoSi_2$ oxidation.) Only when the moving specie is known can the data from the radioactive tracer be interpreted correctly (see, for example, Ref. 8). In cases where two species diffuse, two tracer experiments with radioactive metal and Si should be conducted following an inert marker experiment. Under the assumption that only one process dominates per specie, it is then possible to classify the diffusion process into folding mechanism or lattice diffusion for each species separately.

APPENDIX B

The detailed calculation of the energy scale for possible marker shifts was done as follows. We generally designated the silicide as M_xSi. For $CoSi_2$ and $NiSi_2$, $x = 0.5$; for PdSi, $x = 1$; and for Pd_2Si, $x = 2$. We used the notation of Ref. 16. All the calculations were done for the W marker.

The energy shift with respect to the initial marker energy is calculated using the surface energy approximation for the combined SiO_2 and silicide layers which are on top of the marker. This assumption leads to the linear equation

$$\Delta E = N^{SiO_2} \times d_{ox} \times \Delta\,[\epsilon_0], \tag{1}$$

where d_{ox}, oxide thickness, is taken as 1000 Å for normalization $\Delta\,[\epsilon_0]$ is evaluated for each of the following cases, and is fixed for a given beam energy. Therefore, ΔE for different oxide thicknesses scales linearly with d_{ox}. For the molecular density N^{SiO_2} of SiO_2, we used 2.28×10^{22} cm^{-3}, and the vapor value for the oxygen stopping power[18] which might give small (less than 8%) systematic error.

(1) Silicide is dissociated at the SiO_2 interface; the dissociated metal $M_{sil/ox}$ diffuses to the substrate (a single moving species).

$$M_x\text{Si} + O_2 \rightarrow xM_{sil/ox} + SiO_2. \tag{2}$$

The added stopping power per O_2 is

$$\Delta\,[\epsilon_0] = 2[\epsilon_0]^O_W - x[\epsilon_0]^M_W. \tag{3}$$

The numerical evaluation gives ΔE_1.

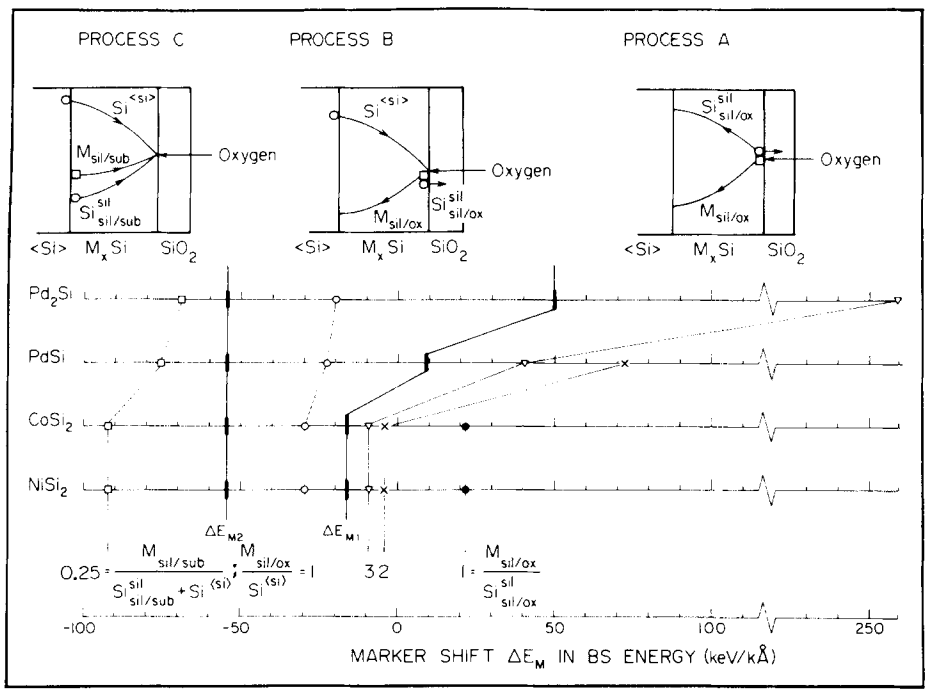

FIG. 10. Energy scale for the shift of a heavy marker (Xe or W) in a 2 MeV $^4He^+$ BS spectrum following oxidation of PdSi, Pd_2Si, $CoSi_2$, and $NiSi_2$. The shifts are calculated per 1000 Å of grown oxide. (See Fig. 2 for schematic description.)

(2) Silicon from the substrate $Si^{\langle Si\rangle}$ diffuses to the SiO_2 interface (a single moving species)

$$Si^{\langle Si\rangle} + M_xSi + O_2 \rightarrow M_xSi + SiO_2. \tag{4}$$

The added stopping power per O_2 is

$$\Delta[\epsilon_0] = 2[\epsilon_0]^O_W + [\epsilon_0]^{Si}_W. \tag{5}$$

The numerical evaluation gives ΔE_2.

(3) Dissociation of the silicide at the silicide/SiO_2 interface. Both metal $M_{sil/ox}$ and silicon $Si^{sil}_{sil/ox}$ from the interface move to the substrate (process A in Fig. 2). We calculate the marker shift for three ratios of $M_{sil/ox}/Si^{sil}_{sil/ox}$. (NOTE: $x < M_{sil/ox}/Si^{sil}_{sil/ox} \leqslant \infty$. The case $M_{sil/ox}/Si^{sil}_{sil/ox} = \infty$ is considered already in no. (1) above).

$$M_{sil/ox}/Si^{sil}_{sil/ox} = r; \quad r = 3; 2; 1; 0.5^*.$$

(*$r = 0.5$ applies only to M_2Si; $r = 1$ applies to M_2Si and MSi only).

$$\left(\frac{r}{r-x}\right)M_xSi + O_2 \rightarrow \left(\frac{x}{r-x}\right)(rM_{sil/ox} + Si^{sil}_{sil/ox}) + SiO_2. \tag{6}$$

The added stopping power per O_2 is

$$\Delta[\epsilon_0] = 2[\epsilon_0]^O_W - \frac{x}{r-x}\{r[\epsilon_0]^M_W + [\epsilon_0]^{Si}_W\} \tag{7}$$

(4) Dissociation of the silicide at the silicide/SiO_2 interface; the dissociated metal $M_{sil/ox}$ diffuses to substrate, and Si from substrate, $Si^{\langle Si\rangle}$, diffuses to SiO_2. (Process B in Fig. 2.) We considered only the ratio $M_{sil/ox}/Si^{\langle Si\rangle} = 1$. (The case $M_{sil/ox}/Si^{\langle Si\rangle} = \infty$ was calculated in no. (1) above, and the case $M_{sil/ox}/Si^{\langle Si\rangle} = 0$ was calculated in point no. (2) above.)

$$\left(\frac{x}{1+x}\right)Si^{\langle Si\rangle} + \left(\frac{1}{1+x}\right)M_xSi + O_2 \rightarrow \left(\frac{x}{1+x}\right)M_{sil/ox} + SiO_2. \tag{8}$$

The added stopping power per O_2 is

$$\Delta[\epsilon_0] = 2[\epsilon_0]^O_W + \frac{x}{1+x}\{[\epsilon_0]^{Si}_W - [\epsilon_0]^M_W\}. \tag{9}$$

(5) Dissociation of the silicide at the $\langle Si\rangle$/silicide interface; the dissociation products as well as substrate diffuse to the silicide/SiO_2 interface where the silicide reconstructs again in front of the marker. (Process C in Fig. 2.) We considered the flux ratio

$$M_{sil/sub}/(Si^{\langle Si\rangle} + Si^{sil}_{sil/sub}) = 0.25.$$

(NOTE: $0 \leqslant M_{sil/sub}/(Si^{\langle Si\rangle} + Si^{sil}_{sil/sub}) < x$.)

$$\left(\frac{x}{x-0.25}\right)Si^{\langle Si\rangle} + Si^{sil}_{sil/sub}) + \left(\frac{x}{4x-1}\right)M_{sil/sub} + O_2 \rightarrow \left(\frac{1}{4x-1}\right)M_xSi + SiO_2. \tag{10}$$

The added stopping power is

$$\Delta[\epsilon_0] = 2[\epsilon_0]^O_W + \left(\frac{x}{4x-1}\right)\{4[\epsilon_0]^{Si}_W + (\epsilon)^M_W\}. \tag{11}$$

In Fig. 10, we give the calculated values for each of the silicides we investigated, using the W marker. Since the accuracy of our measurement and analysis is not better than 10%, we used this value for the Xe marker as well. (This contributes 3% error in the worst case.) Any heavy marker should result in almost the same marker shift. All the values are given for a 2 MeV analyzing $^4He^+$ beam and a 170° scattering angle.

The above model applies for marker shift as long as the

final marker position is inside the silicide. When the reaction progresses further such that the marker reaches an interface, the fate of the marker is determined by the energetics and kinetics of the marker at that interface. It is nontheless possible to conclude if dissociation at the silicide/SiO_2 interface occurs or not, because dissociation is necessary for the marker to reach the SiO_2 interface.

[1]M-A. Nicolet and S. S. Lau, in VLSI *Electronics, Microstructure Science*, series, edited by N. Einspruch, (G. Larrabee, Guest Editor, Academic, New York, 1983). Vol. 6., Chap. 6.
[2]M. Bartur and M-A. Nicolet, Appl. Phys. A **29**, 69 (1982).
[3]M. Bartur and M-A. Nicolet, (unpublished).
[4]M. Bartur and M-A. Nicolet, (unpublished).
[5]R. Pretorius, C. L. Ramiller, and M-A. Nicolet, Nucl. Instrum. Methods **149**, 629 (1978).
[6]R. Pretorius, J. Electrochem. Soc. **128**, 107 (1981).
[7]A. P. Botha and R. Pretorius, Thin Solid Films, **93**, 127 (1982).
[8]J. E. E. Baglin, A. H. Atawater, D. Gupta, and F. M. d'Heurle, Thin Solid Films, **93**, 255 (1982).
[9]A. G. Cullis, T. E. Seidel, and R. L. Meek, J. Appl. Phys. **49**, 5188 (1978).
[10]M. Wittmer, J. Roth, P. Revesz, and J. W. Mayer, J. Appl. Phys. **49**, 5207 (1978).
[11]M. Bartur and M-A. Nicolet, Appl. Phys. Lett. **40**, 175 (1982).
[12]D. M. Scott, (private communication).
[13]R. Pretorius, W. Strydom, J. W. Mayer, and C. Comrie, Phys. Rev. B **22**, 1885 (1980).
[14]G. J. van Gurp, D. Sigurd, and W. F. van der Weg, Appl. Phys. Lett. **29**, 159 (1976).
[15]F. d'Heurle, S. Petersson, L. Stolt, and B. Stritzker, J. Appl. Phys. **53**, 5678 (1982).
[16]J.-R. Chen, Y.-C. Liu, and S.-D. Chu, Appl. Phys. Lett. **40**, 263 (1982).
[17]D. Shaw, *Atomic Diffusion in Semiconductors*, (Plenum, New York, 1973).
[18]W. K. Chu, J. W. Mayer, and M-A. Nicolet, *Backscattering Spectrometry*, (Academic, New York, 1978).